Drug-target residence time : a case for the adenosine A1 and A2A receptors

Guo, D.

Chapter 3

Dual-point competition association assay A fast and high-throughput kinetic screening method for assessing ligand-receptor binding kinetics

Guo D, Van Dorp EJ, Mulder-Krieger T, Van Veldhoven JPD, Brussee J, IJzerman AP, Heitman LH.
Adapted from: *J Biomol Screen* 2013;18(3):309-320.

About this chapter

This chapter introduces a method that enables fast and large format kinetics screening—the dual-point competition association assay. It measures radioligand binding at two different time points in the absence or presence of unlabeled competitors. This assay yields the kinetic rate index (KRI), which is a measure for the binding kinetics of the unlabeled ligands screened. As a prototypical drug target the adenosine A_1 receptor (A_1R) was chosen for assay validation and optimization. A screen with 35 high affinity A_1R antagonists yielded seven compounds with a KRI-value above 1.0, which indicated a relatively slow dissociation from the target. All other compounds had a KRI-value below or equal to 1.0, predicting a relatively fast dissociation rate. Several compounds were selected for follow-up kinetic quantifications in classical kinetic assays and were shown to have kinetic rates that corresponded to their KRI-values. The dual-point assay and KRI-value may have general applicability at other GPCRs, and at drug targets from other protein families.

3.1 Introduction

The traditional paradigm of drug discovery places an emphasis on dose-dependent assessments (i.e., affinity or potency) to identify lead compounds, which are usually performed under equilibrium conditions.[1,2] With this approach ligand-receptor binding kinetics are usually overlooked. However, the importance of this latter aspect is increasingly recognized, since several lines of research have retrospectively suggested that the binding kinetics, especially the lifetime of the ligand-receptor interaction, is a critical differentiator and predictor for drug efficacy and safety.[1-5] This emerging paradigm shift from a classical affinity-based approach emphasizes ligand-receptor residence time (RT, the reciprocal of the dissociation rate constant k_{off}),[6] which is a measure for the duration that a ligand stays in complex with its target.

In this chapter we introduce an assay to perform kinetic binding screens, namely the dual-point competition association assay. This method is based on the theory developed by Motulsky and Mahan, where an unlabeled competitor is co-incubated with a radioligand during a kinetic association experiment.[11] If the competitor dissociates faster from its target than the radioligand, the specific binding of the radioligand will slowly and monotonically approach its equilibrium in time (Figure 3.1, Curve C). However, when the competitor dissociates slower, the association curve of the radioligand will consist of two phases starting with a typical 'overshoot' and then a decline until a new equilibrium is reached (Figure 3.1, Curve B). In the dual-point competition association assay, we select two time points to measure radioligand binding: 1) at which the radiolabeled ligand just reaches equilibrium under control conditions in the absence of an unlabeled ligand (Figure 3.1, Curve A and t_1), and 2) at which the incubation time is long enough for the labeled and unlabeled compound to equilibrate with the target (Figure 3.1, Curve B and C, t_2). Next, we calculate the ratio of the binding at the first time point (B_{t1}) and that at the second time point (B_{t2}), which we define as the 'kinetic rate index' (KRI) value for a certain unlabeled compound. In this manner, the compounds that quickly dissociate from their target will have a ratio below or equal to one (Figure 3.1, Curve C). Conversely, compounds that dissociate slowly from their target, compared to the radioligand used, will have a KRI value larger than one, resulting from the typical 'overshoot' in the association curve (Figure 3.1, Curve B).

In the present chapter, we have used the adenosine A_1 receptor (A_1R)

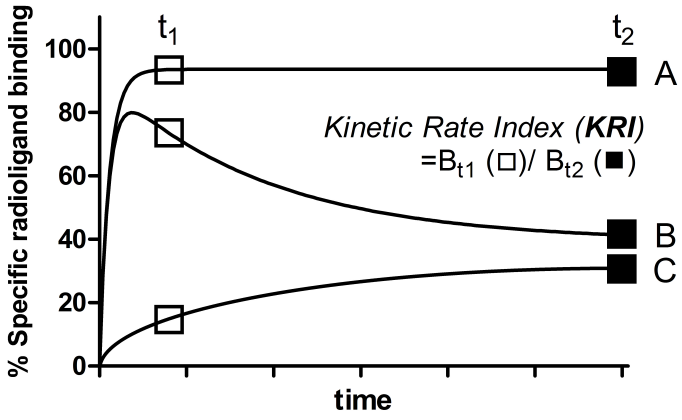

Figure 3.1 | Schematic presentation of the background for the dual-point competition association assay. Curve A: a radioligand association curve without a co-incubation of unlabeled competitor. Curve B: a co-incubated unlabeled competitor dissociates slower than the radioligand used ($k_2 > k_4$). Curve C: a co-incubated unlabeled competitor dissociates faster than the radioligand used ($k_2 < k_4$). B_{t1}: specific radioligand binding at the first time point (t_1); B_{t2}: specific radioligand binding at the second time point (t_2). Kinetic rate index (KRI) is defined as B_{t1} / B_{t2}.

as a prototypic target to illustrate the utility of the dual-point competition association screening method and the resulting KRI-values. The adenosine A_1R is one of four adenosine receptors subtypes (i.e., A_1, A_{2A}, A_{2B} and A_3 receptors), which belong to the superfamily of G protein-coupled receptors (GPCRs).[12,13] The A_1R is a promising therapeutic target, since it has clinical relevance in neurological disorders, such as cognition deficits, and is involved in cardiovascular preconditioning.[14,15] A tool compound, namely FSCPX (Figure 3.5), was used to set up the dual-point screening assay, since it is a known irreversibly binding antagonist for the A_1R.[16] In total 35 in-house synthesized A_1R antagonists were screened using the dual-point competition association assay.[17,18] Eight compounds with divergent KRI values were selected for extensive kinetic assessments. Moreover, we decided to radiolabel one of the slowly dissociating antagonists, namely LUF5962 (compound **31**, Figure 3.5),[17] tested its binding kinetics in traditional kinetic association and dissociation assays to validate the results from our dual-point screening assay, and used it subsequently to profile the same panel of 35 compounds.

3.2 Materials and methods

Chemicals and reagents

[^{3}H]-1,3-dipropyl-8-cyclopentyl-xanthine ([^{3}H]-DPCPX, specific activity 116.7 Ci/mmol) was purchased from ARC Inc. (St. Louis, USA). Adenosine deaminase (ADA) was purchased from Boehringer Mannheim (Mannheim, Germany). CHAPS [3-((3-cholamidopropyl)-dimethylammonio)-1-propanesulfonate)] were obtained from Carl Roth GmbH (Karlsruhe, Germany). DPCPX (selective A_1R antagonist[31]), PEI (Polyethyleneimine) and bovine serum albumin (BSA) were from Sigma (St. Louis, MO, U.S.A). Bicinchoninic acid (BCA) and BCA protein assay reagent were obtained from Pierce Chemical Company (Rockford, IL, U.S.A.). All 35 A_1R antagonists were synthesized in our laboratory as described previously.[17,18] Chinese hamster ovary cells stably expressing the hA_1R were obtained from Prof. Steve Hill (University of Nottingham, UK). All other chemicals were of analytical grade and obtained from standard commercial sources.

Preparation of [^{3}H]-LUF5962

[^{3}H]-8-cyclopentyl-2,6-diphenyl-9H-purine ([^{3}H]-LUF5962, specific activity 51.7 Ci/mmol) was customly labeled by RC Tritec (Teufen, Switzerland). Unlabeled LUF5962 was provided as a dehydrogenenated precursor compound, namely 8-cyclopent-3-en-1-yl-2,6-diphenyl-9H-purine. This compound was dissolved in ethanol, 10% Pd/C was added to the solution, and the reaction mixture was tritiated with tritium gas. After removal of labile tritium and purification by HPLC, the one-stage synthesis yielded [^{3}H]-LUF5962 with a specific activity of 54.0 Ci/mmol (2.0 TBq/mmol). The radiochemical purity was > 97%, as determined by HPLC.

[^{3}H]-LUF5962 binding assay optimization

The assay conditions for [^{3}H]-LUF5962 binding to CHOhA$_1$R membranes were optimized according to a general radioligand binding protocol in our laboratory.[21] Initial experiments were performed with 1.0 nM (approximately 12,000 DPM) [^{3}H]-LUF5962 and 5 µg of CHOhA$_1$R membranes in a simple buffer of low ionic strength (25 mM Tris-HCl, pH 7.4) to which 5 mM $MgCl_2$ was added. Next, we studied further buffer components, filters, filter pretreatment and different radioligand and membrane concentrations to improve the window of specific binding. Firstly, a relatively low concentration (1.0 nM) of [^{3}H]-LUF5962 was enough for an appreciable window of specific binding, which was improved by the addition of 0.1% CHAPS due to a decrease in non-specific binding, while the addition of 0.1% BSA had no effect. Secondly, coating GF/B or GF/C glass fiber filters with PEI to separate free from membrane-bound radioligand did not significantly reduce the non-specific binding (data not shown). Taken together, it was decided to add 0.1% CHAPS in the assay buffer, use uncoated GF/B filters and 5 µg of membranes to yield a desired window of approximately 2000 DPM. Total binding of the radioligand was around 35% of the amount added and thus resulted in radioligand depletion that was unavoidable due to relatively high non-specific binding of [^{3}H]-LUF5962 even under optimized conditions. Finally, initial kinetic association experiments taught us that the optimal incubation time to reach equilibrium was 30 min at 25 °C.

Cell culture and membrane preparation

Chinese hamster ovary cells stably expressing the human adenosine A_1 receptor (CHOhA$_1$R) were grown in Ham's F12 medium containing 10% (v/v) normal adult bovine serum, streptomycin (100 µg/mL), penicillin (100 IU/mL), and G418 (0.4 mg/mL) at 37 ˚C in 5% CO_2. Cells were subcultured twice weekly at a ratio of 1:20 on 10 cm ø culture plates. For membrane preparation, cells were subcultured 1:10 and then transferred to 15 cm ø plates. Cells grew to 80%-90% confluency were detached from plates by scraping them into 5 mL PBS, collected and centrifuged at 700 × g (3000 r.p.m.) for 5 min. Cell pellets derived from 30 plates were pooled and resuspended in 20 mL of ice-cold 25 mM Tris-HCl buffer, pH 7.4. An UltraThurrax (Heidolph Instruments, Schwabach, Germany) was used to homogenize the cell suspension. Membranes and the cytosolic fraction were

separated by centrifugation at 100,000 × g (31,000 r.p.m.) in a Beckman Optima LE-80K ultracentrifuge (Beckman Coulter, Fullerton, CA) at 4 ˚C for 20 min. The pellet was resuspended in 15 mL of the Tris-HCl buffer and the homogenization and centrifugation step was repeated. Tris-HCl buffer (10 mL) was used to resuspend the pellet and ADA was added (0.8 IU/mL) to break down endogenous adenosine. Membranes were stored in 250 µL aliquots at -80 ˚C. Concentrations of the membrane protein were measured using the BCA method.[19]

Radioligand saturation and displacement assays

Membrane aliquots containing 5 µg of protein were incubated in a total volume of 100 µL of assay buffer [25 mM Tris-HCl, pH 7.4, supplemented with 5 mM $MgCl_2$ and 0.1% (w/v) CHAPS] at 25 ˚C for one hour ([^{3}H]-DPCPX) or three hours ([^{3}H]-LUF5962). Notably, optimal incubation times were determined with Equation 5 under *Data analysis*, which ensured that binding of the radioligand at the lowest concentration also reached equilibrium. For saturation experiments, a range of concentrations of [^{3}H]-DPCPX (~0.2-20 nM) or [^{3}H]-LUF5962 (~0.1-13 nM) was used, respectively. In an initial experiment, nonspecific binding was determined at twelve concentrations of radioligand (i.e., [^{3}H]-DPCPX ~0.2-20 nM and [^{3}H]-LUF5962 ~0.1-13 nM) in the presence of 100 µM N^6-cyclopentyladenosine (CPA, selective A_1R agonist[32]). Since the nonspecific binding of both radioligands proved to be linear for these concentrations ($r^2 > 0.95$, $P < 0.0001$, data not shown), it was decided to use only three, evenly spaced, concentrations of radioligand to determine nonspecific binding in following saturation experiments. Displacement experiments were performed using eleven concentrations of competing ligands in the presence of 2.5 nM [^{3}H]-DPCPX. At this concentration, total radioligand binding did not exceed 10% of that added to prevent ligand depletion. Nonspecific binding was determined in the presence of 100 µM CPA. Incubations were terminated by rapid vacuum filtration to separate the bound and free radioligand through 96-well GF/B filter plates using a Perkin Elmer Filtermate-harvester (Perkin Elmer, Groningen, Netherlands) or through Whatman GF/B filters (Whatman International, Maidstone, UK) using a Millipore manifold (Millipore, Billerica, MA, USA). Filters were subsequently washed three times with ice-cold wash buffer (25

mM Tris-HCl, pH 7.4, supplemented with 5 mM $MgCl_2$). The filter-bound radioactivity was determined by scintillation spectrometry using the P-E 1450 Microbeta Wallac Trilux scintillation counter (Perkin Elmer, Groningen, Netherlands) for 96-well GF/B filter plates or by a liquid scintillation counter (Tri-Carb 2900 TR, Perkin-Elmer) for Whatman GF/B filters.

Radioligand association and dissociation assays

Association experiments were performed by incubating membrane aliquots containing 5 μg of protein in a total volume of 100 μL of assay buffer at 25 °C with 2.5 nM [^{3}H]-DPCPX or 1.0 nM [^{3}H]-LUF5962. The amount of radioligand bound to the receptor was measured at different time intervals during a total incubation of 20 min for [^{3}H]-DPCPX or one hour for [^{3}H]-LUF5962. Dissociation experiments were performed by pre-incubating membrane aliquots containing 5 μg of protein in a total volume of 100 μL of assay buffer either for 20 min for [^{3}H]-DPCPX or for one hour for [^{3}H]-LUF5962. After the pre-incubation, radioligand dissociation was initiated by the addition of 10 μM unlabeled CPA. The amount of radioligand still bound to the receptor was measured at various time intervals for a total of one hour for [^{3}H]-DPCPX or two hours for [^{3}H]-LUF5962 to ensure that they were fully dissociated from hA_1R. Incubations were terminated and samples were obtained as described under *Radioligand saturation and displacement assays.*

Competition association assay

The binding kinetics of unlabeled ligands was quantified using the competition association assay based on the theoretical framework by Motulsky and Mahan.[11] In the standard assay, three different concentrations of unlabeled DPCPX were tested, namely at 0.3-, 1- and 3-fold its K_i. For unlabeled LUF5962, 1-, 3- and 10-fold its K_i were used, while for FSCPX, 3-, 10- and 30-fold its K_i were used. In the simplified one-concentration competition association assay, only a concentration of 10-fold of the K_i value was used to determine the binding kinetics of unlabeled ligands. The competition association assay was initiated by adding membrane aliquots (5

μg/well) at different time points for a total of 90 min to a total volume of 100 μL of assay buffer at 25 °C with 2.5 nM [^{3}H]-DPCPX in the absence or presence of competing ligand (10-fold K_i). Only for FSCPX the assay time was increased to 180 min. Incubations were terminated and samples were obtained as described under *Radioligand saturation and displacement assays*.

Dual-point competition association assay

The dual-point competition association experiments were performed by incubating membrane aliquots containing 5 μg of protein for 15 min or 120 min in a total volume of 100 μL of assay buffer with 2.5 nM [^{3}H]-DPCPX and for 30 min or 120 min with 1.0 nM [^{3}H]-LUF5962 in the absence or presence of unlabeled ligands. The amount of radioligand bound to the receptor was measured after co-incubation of the unlabeled A_1R antagonists at 10-fold their respective K_i values. Incubations were terminated after either 15 min or 120 min for [^{3}H]-DPCPX and 30 min or 120 min incubation for [^{3}H]-LUF5962 and samples were obtained as described under *Radioligand saturation and displacement assays*. Kinetic rate index (KRI) values of unlabeled ligands were calculated by using Equation 6 as mentioned below in *Data analysis*.

Data analysis

All experimental data was analyzed by using GraphPad Prism 5.0 (GraphPad Software Inc., San Diego, CA). All values obtained are means of at least three independent experiments performed in duplicate. K_D and B_{max} values of [^{3}H]-DPCPX or [^{3}H]-LUF5962 at hA_1R membranes were obtained by computational analysis of saturation curves. IC_{50} values obtained from competition displacement binding data were converted into K_i values using the Cheng-Prusoff equation.[20] Association data was fitted using *one phase exponential association* as follows:

$$Y = Y_{\max} \cdot (1 - e^{-k_{obs} \cdot t}) \quad (1)$$

Where t is a given time, Y is the amount of specific radioligand binding, Y_{max} the specific radioligand binding at equilibrium, k_{obs} the observed rate constant to approach equilibrium. The time for a radioligand to reach half of the Y_{max} ($t_{1/2,\ association}$, the association half-life) is

$$t_{1/2,association} = \frac{\ln 2}{k_{obs}} \tag{2}$$

Values for k_{on} were obtained by converting k_{obs} values as follows:

$$k_{on} = \frac{k_{obs} - k_{off}}{[radioligand]} \tag{3}$$

where k_{off} was determined in independent dissociation experiments. Dissociation data was fitted using *one phase exponential decay*.

In the dual-point competition association assay, t_1 was set at the time that radioligand binding just reached equilibrium. Specifically, we have defined the time to reach equilibrium, when 99.5% of total binding was reached, i.e., at 8-fold the association half-life. Thus,

$$t_1 = 8 \cdot t_{1/2,association} \tag{4}$$

Taken together, t_1 was determined by combining Equations 2, 3 and 4 as follows:

$$t_{1/2,association} = \frac{\ln 2}{k_{on} \cdot [radioligand] + k_{off}} \tag{5}$$

The second time point (t_2) was arbitrarily set at a time long enough for the binding of the unlabeled ligand to reach a plateau. KRI (kinetic rate index) values were calculated by dividing the specific radioligand binding measured at t_1 (B_{t1}) by its binding at t_2 (B_{t2}) in the presence of unlabeled competing ligands as follows:

$$KRI = \frac{B_{t_1}}{B_{t_2}} \tag{6}$$

Association and dissociation rates for unlabeled ligands were calculated by fitting the data in the competition association model using '*kinetics of competitive binding*' in Prism 5 as follows:[11]

$$
\begin{aligned}
K_A &= k_1 \cdot [L] \cdot 10^{-9} + k_2 \\
K_B &= k_3 \cdot [I] \cdot 10^{-9} + k_4 \\
S &= \sqrt{(K_A - K_B)^2 + 4 \cdot k_1 \cdot k_3 \cdot L \cdot I \cdot 10^{-18}} \\
K_F &= 0.5 \cdot (K_A + K_B + S) \\
K_S &= 0.5 \cdot (K_A + K_B - S) \\
Q &= \frac{B_{\max} \cdot k_1 \cdot L \cdot 10^{-9}}{K_F - K_S} \\
Y &= Q \cdot \left(\frac{k_4 \cdot (K_F - K_S)}{K_F \cdot K_S} + \frac{k_4 - K_F}{K_F}(-K_F \cdot X) - \frac{k_4 - K_S}{K_S} e^{(-K_S \cdot X)}\right)
\end{aligned}
\tag{7}
$$

where X is the time (min), Y is the specific binding (DPM), k_1 the k_{on} ($M^{-1} \cdot min^{-1}$) of [^{3}H]-DPCPX predetermined in association experiments, k_2 the k_{off} (min^{-1}) of [^{3}H]-DPCPX predetermined in dissociation experiments, L the concentration of [^{3}H]-DPCPX used (nM), B_{max} the total binding (DPM) and I the concentration of unlabeled ligand (nM). Fixing these parameters into Equation 7 allows the following parameters to be calculated: k_3 is the k_{on} ($M^{-1} \cdot min^{-1}$) of the unlabeled ligand and k_4 is the k_{off} (min^{-1}) of the unlabeled ligand. The association and dissociation rates were used to calculate the 'kinetic K_D' as follows:

$$K_D = \frac{k_{off}}{k_{on}} \tag{8}$$

3.3 Results and discussion

Quantification of the K_D and B_{max} of [^{3}H]-DPCPX and [^{3}H]-LUF5962 in saturation binding experiments

Saturation binding experiments were performed with [^{3}H]-DPCPX and [^{3}H]-LUF5962 at 25°C. Both [^{3}H]-DPCPX and [^{3}H]-LUF5962 bound saturably and specifically to a single class of binding sites at CHOhA_1R membranes. The K_D value of [^{3}H]-DPCPX obtained from the saturation experiments was

2.5 ± 0.1 nM and the B_{max} value was 14.0 ± 1.0 pmol/mg protein, while the K_D value of [^{3}H]-LUF5962 was 0.83 ± 0.08 nM and the B_{max} was 17.1 ± 0.9 pmol/mg protein (Table 3.1). It should be kept in mind that ligand depletion was an issue when using [^{3}H]-LUF5962, and thus it represents a less than ideal radioligand. However, in the paragraphs below we discuss that it can still be effectively used in the kinetic characterization of unlabeled ligands. The K_D value for [^{3}H]-DPCPX obtained in this experiment was in line with the K_D value reported previously.[21] This K_D was used to derive K_i values from IC_{50} values for unlabeled ligands (see below).

Quantification of the association [k_{on} (k_1)] and dissociation rates [k_{off} (k_2)] of [^{3}H]-DPCPX and [^{3}H]-LUF5962 at CHOhA$_1$R membranes

Receptor association [k_{on} (k_1)] and dissociation rates [k_{off} (k_2)] of [^{3}H]-DPCPX and [^{3}H]-LUF5962 were determined in standard radioligand association and dissociation experiments. Association and dissociation assays were conducted at 25 ˚C for both radioligands. The observed association rates (k_{obs}) were converted to k_{on} values by using Equation 3 described in *Methods*. The binding of [^{3}H]-DPCPX and [^{3}H]-LUF5962 approached equilibrium after approximately 15 and 30 min, respectively (Figure 3.2). Both [^{3}H]-DPCPX and [^{3}H]-LUF5962 had relatively fast association rates of 0.20 ± 0.01 $nM^{-1}\cdot min^{-1}$ and 0.13 ± 0.01 $nM^{-1}\cdot min^{-1}$, respectively. Binding of both radioligands was reversible after the addition of 10 μM CPA and complete dissociation was reached after approximately 25 min for [^{3}H]-DPCPX and 120 min for [^{3}H]-LUF5962 (Figure 3.2). The dissociation rate of [^{3}H]-LUF5962 was eight-fold lower than that of [^{3}H]-DPCPX from the hA$_1$R (Figure 3.2 and Table 3.1). The dissociation binding constants (kinetic K_D) of the radioligands were derived from the dissociation and association rates. [^{3}H]-LUF5962 had an approximately five-fold higher affinity than [^{3}H]-DPCPX, 0.20 ± 0.02 nM compared to 1.1 ± 0.1 nM, respectively.

Quantification of the affinity (K_i) of A$_1$R ligands in displacement experiments

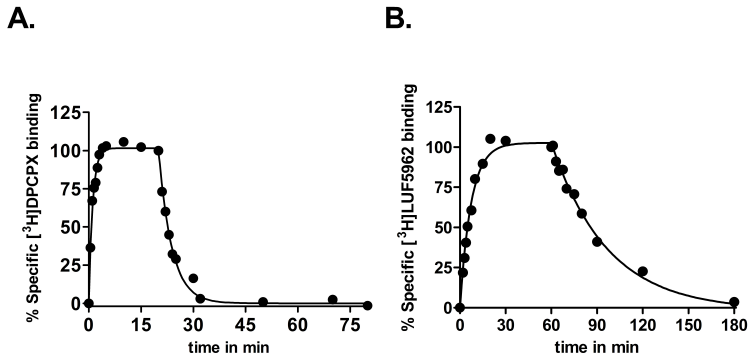

Figure 3.2 | Association and dissociation kinetics of [^{3}H]-DPCPX (Panel A) and [^{3}H]-LUF5962 (Panel B) at 25 ˚C to and from human adenosine A_1 receptors stably expressed on CHO membranes. Association data was fitted in Prism 5.0 using *one-phase exponential association*. Values for k_{on} were obtained by using Equation 3. Dissociation data was fitted using *one-phase exponential decay*. Representative graphs from one experiment performed in duplicate.

Displacement experiments with several A_1R ligands were performed at 25 ˚C to determine their affinities for the hA_1R. The tested hA_1R antagonists showed concentration-dependent inhibition of specific [^{3}H]-DPCPX binding and the data was best fitted to a one-site competition model. Unlabeled DPCPX and LUF5962 had affinities of 2.3 ± 0.3 nM and 0.24 ± 0.03 nM, respectively (Table 3.1). Affinities of other antagonists shown in Table 3.2 were taken from previously published in-house experiments.[17,18]

Validation and optimization of the competition association assay at the hA_1R

With the pre-characterized k_{on} (k_1) and k_{off} (k_2) values of [^{3}H]-DPCPX binding from direct association and dissociation experiments, k_{on} (k_3) and k_{off} (k_4) values of unlabeled DPCPX and LUF5962 were determined by fitting the values into Equation 7 described in *Methods*. Three different concentrations of the unlabeled reference compounds (DPCPX and LUF5962) were tested

Table 3.1 | Comparison of the affinity and kinetic rates of DPCPX and LUF5962 obtained in different radioligand binding assays.

Cmpd	*K_D (nM)*[a]	*K_i (nM)*[b]	*k_{on} ($nM^{-1}\cdot min^{-1}$)*[c]	*k_{off} (min^{-1})*[d]	*Kinetic K_D (nM)*[e]
DPCPX	2.5 ± 0.1	2.3 ± 0.3	0.20 ± 0.01	0.21 ± 0.01	1.1 ± 0.1
LUF5962	0.83 ± 0.08	0.24 ± 0.03	0.13 ± 0.01	0.025 ± 0.002	0.20 ± 0.02

Values are means ± s.e.m of at least three independent experiments performed in duplicate. [a] [^{3}H]-DPCPX (~0.2-20 nM) or [^{3}H]-LUF5962 (~0.1-13 nM) saturation binding to $CHOhA_1$ membranes at 25 ˚C. [b] from displacement of specific [^{3}H]-DPCPX binding from $CHOhA_1$ membranes at 25 ˚C. [c] Association [k_{on} (k_1)] of [^{3}H]-DPCPX or [^{3}H]-LUF5962 to $CHOhA_1R$ membrane at 25 ˚C. [d] Dissociation [k_{off} (k_2)] of [^{3}H]-DPCPX or [^{3}H]-LUF5962 from $CHOhA_1R$ membrane at 25 ˚C. [e] Kinetic $K_D = k_{off} / k_{on}$. k_{on} (k_1) values were generated from [^{3}H]-DPCPX (2.5 nM) or [^{3}H]-LUF5962 (1.0 nM) association assays; k_{off} (k_2) values were generated from [^{3}H]-DPCPX (2.5 nM) or [^{3}H]-LUF5962 (1.0 nM) dissociation assays at 25 ˚C.

(Figure 3.3). Their k_{on} (k_3) and k_{off} (k_4) values determined by the competition association method were 0.14 ± 0.02 $nM^{-1}\cdot min^{-1}$ and 0.25 ± 0.01 min^{-1} for unlabeled DPCPX (Figure 3.3A, Table 3.2), and 0.060 ± 0.010 $nM^{-1}\cdot min^{-1}$ and 0.021 ± 0.005 min^{-1} for LUF5962 (Figure 3.3B, Table 3.2), which were in accordance with the k_1 and k_2 values determined in 'traditional' association and dissociation experiments (Figure 3.2 and Table 3.1). Comparison of the dissociation constants and affinities obtained from the different equilibrium and kinetic experiments (Table 3.1) further verified that the competition association assay could be accurately used to determine the binding kinetics of unlabeled A_1R ligands.

Optimization of the dual-point competition association assay at the hA_1R

For the dual-point competition association assay it was necessary to decide on the optimal compound concentration and the two time points (t_1 and t_2) to obtain a robust kinetic screening assay. Therefore, we decided to optimize the assay using the reference antagonist FSCPX as a positive control, which is known to bind irreversibly to the hA_1R.[16]

Firstly, we used concentrations that represented 3-, 10- and 30-fold K_i values of unlabeled FSCPX to study the influence of different concentrations on the kinetic assay. It follows from Figure 3.4A that a long incubation time

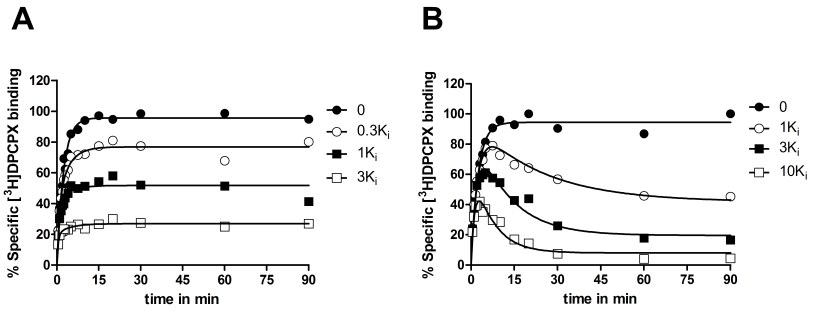

Figure 3.3 | Validation and optimization of the competition association assay at the hA_1R. Competition association assay with [^{3}H]-DPCPX at 25 ˚C from human adenosine A_1 receptors stably expressed on CHO membranes in the absence or presence of 0.3-fold, one-fold and three-fold K_i value of unlabeled DPCPX (Panel A) or one-fold, three-fold and ten-fold K_i value of LUF5962 (Panel B). Association and dissociation rates for unlabeled ligands were calculated by fitting the data in the competition association model as in Equation 7.[11] Representative graph from one experiment performed in duplicate.

(i.e., 180 min) is needed for FSCPX to abrogate all [^{3}H]-DPCPX binding at a low concentration, i.e., 3-fold its K_i value. The co-application of 30-fold its K_i value resulted in a faster knockdown of [^{3}H]-DPCPX binding sites, i.e., after approximately 60 min. Such a significant decrease of [^{3}H]-DPCPX binding reduced the KRI window. Incubation of the membranes with an FSCPX concentration equaling 10 times its K_i value led to an intermediate situation (Figure 3.4A). Notably, the set of three FSCPX concentrations are higher than the concentrations used in experiments with LUF5962 and DPCPX (Figure 3.3). In order to achieve radioligand equilibrium binding as much as possible with slowly dissociating competitors (or irreversibly binding competitors like FSCPX) in the same experimental incubation time, higher concentrations need to be used than for competitors with relatively faster or equal dissociation rates. The latter has also been described for the muscarinic M_3 and histamine H_3 receptor.[9,28] In the present chapter, we observed that 10-fold K_i of the competitor gave reasonably large assay windows for all three ligands displaying divergent off-rates (i.e., DPCPX, LUF5962 and FSCPX). Hence, for screening purposes it was decided to use concentrations equal to 10-fold the K_i values of the respective unlabeled ligands. It is important to note that 10-fold K_i is optimal for A_1R in the current protocol, yet this

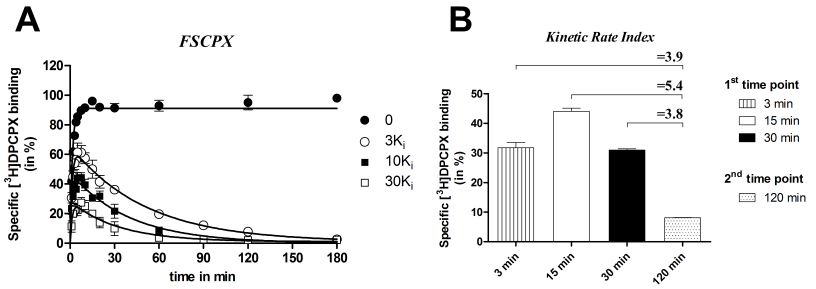

Figure 3.4 | Optimization of the dual-point competition association assay at hA_1R. Competition association assay with [^{3}H]-DPCPX at 25 ˚C from human adenosine A_1 receptors stably expressed on CHO membranes in the absence or presence of 3-fold, 10-fold and 30-fold K_i value of FSCPX (Panel A). Association and dissociation rates for unlabeled FSCPX were calculated by fitting the data in the competition association model using '*kinetics of competitive binding*' in Prism 5 in Equation 7.[11] Kinetic rate indexes of FSCPX calculated from the ratio of specific [^{3}H]-DPCPX binding at 3 min, 15 min or 30 min and its binding at 120 min (Panel B). KRI values were calculated by using Equation 6. Data are shown as mean ± s.e.m from three separate experiments each performed in duplicate.

concentration may not be suitable on other drug targets, especially when divergent concentrations of radioligand are used in the competition association assay. For instance, Dowling and Charlton used approximately 25-fold K_D of the radioligand in their competition association assay on the muscarinic M_3 receptor. This requires higher concentrations of unlabeled ligands (from 10-fold to 1000-fold their respective K_i values) to achieve full resolution of radioligand equilibrium binding within the frame of incubation time.[9] Similarly, Slack *et al.* used higher concentrations of unlabeled ligands (from less than 15-fold to over 200-fold K_i) in their competition association assays on histamine H_1 and H_3 receptors.[28] Therefore, for a general optimization of the dual-point assay on other drug targets, it is suggested that one should take into account the radioligand's concentration, assay incubation time and expected kinetic profiles of the competitors for optimization of the competitors concentration, since all these parameters influence the resolution of the assay.

Secondly, we optimized the two time points (t_1 and t_2). As for t_2 the incubation time was set at 120 min, which was based on the observation in Figure 3.4A that in the presence of an FSCPX concentration of 10-fold its

K_i value [^{3}H]-DPCPX binding was negligible after 120 min incubation. As mentioned above, we assumed that within this time frame most compounds would equilibrate with the target, even if they were kinetically different, as further corroborated by Figure 3.3. As for t_1 the incubation time was set at 15 min, since under control conditions (i.e., absence of unlabeled ligand) [^{3}H]-DPCPX binding reached equilibrium after 15 minutes at 25˚C according to Equation 5 and Figure 3.2A. It was also tried to set t_1 at a much longer (i.e., 30 min) or shorter incubation time (i.e., 3 min). From Figure 3.4B it follows that the selection of t_1 and t_2 clearly affects the KRI values obtained. In other words, a shorter or longer incubation time than 15 min for t_1 reduced its margin over the control (KRI = 1.0), i.e., KRI values = 3.9 or 3.8, respectively, while t_1 = 15 min provided a more significant KRI value of 5.4 for FSCPX. Therefore, incubation times of 15 min (t_1) and 120 min (t_2) were used for the dual-point competition association assay with [^{3}H]-DPCPX at the hA_1R. Notably, it is impossible to define an absolute value or cut-criterion of t_1 and t_2, since the two time point set-up is dependent on several factors (i.e., radioligand concentration, temperature). For a general application on other targets, we suggest that one can start with setting t_1 at a time when the radioligand just reaches equilibrium by using Equation 5, while for t_2 a later time point is chosen long enough for the binding of the unlabeled ligand to reach a plateau. A late t_2 of course compromises the convenience of this screening method, as the total assay time increases. Therefore, it may be necessary to perform similar 'tailored' optimizations of time points and concentrations, and even the choice of the radioligand, to obtain robust results on other drug targets.

Kinetic screening of hA_1R antagonists using dual-point competition association assay

In the present chapter, 35 hA_1R antagonists synthesized in-house[17,18] were screened in the newly developed dual-point competition association assay (Figure 3.5). The specific binding of [^{3}H]-DPCPX was measured after 15 min and 120 min and for [^{3}H]-LUF5962 after 30 min and 120 min in the absence and presence of a single concentration of unlabeled competitive ligand (10-fold K_i, in both [^{3}H]-DPCPX and [^{3}H]-LUF5962 assays). This allowed us to calculate the kinetic rate index (KRI) values for each compound by using

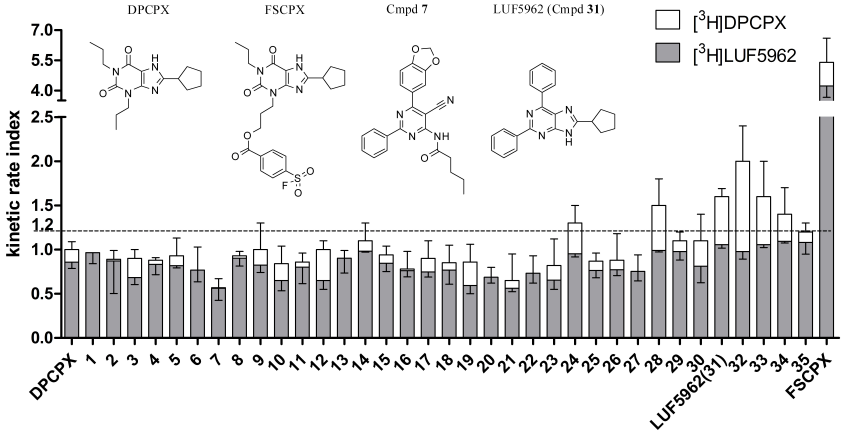

Figure 3.5 | Kinetic rate indexes (KRI) of 35 in-house hA_1R antagonists, DPCPX and FSCPX.[16-18] The KRI values of the same panel of unlabeled ligands against [^{3}H]-LUF5962 (gray bars) are integrated with the results obtained with [^{3}H]-DPCPX (white bars). Values were obtained from the dual-point assays and calculated by using Equation 6. The KRI of the reference compounds, unlabeled DPCPX or LUF5962 (compound **31**), were determined approximately 1.0 in the respective screen. FSCPX was the 'tool compound' and known to bind irreversibly to hA_1R. Seven compounds with a kinetic rate index ≥ 1.2 (the stippled line) were found using [^{3}H]-DPCPX and no compounds with a kinetic rate index ≥ 1.2 were found using [^{3}H]-LUF5962 (excluding FSCPX in both cases). Data are shown as mean ± s.e.m from three separate experiments each performed in duplicate. Chemical structures of DPCPX, FSCPX, compound **7** and LUF5962 (compound **31**) are also presented.

Equation 6. The KRI cut-off value for kinetically interesting compounds was arbitrarily set at 1.2 (Figure 3.5, the stippled line) rather than 1.0 to avoid false positives. It is worth mentioning that the cut-off value for the KRI can be flexible based on a different screening purpose. In other words, one can specifically set it higher to select only longer residence time compounds or lower to obtain more hits for future chemical modifications. In the present chapter, most compounds were found to have KRI values equal to or less than one (Figure 3.5) with both radioligands, which were thus considered to have similar or faster off-rates from the hA_1R compared to the radioligands used, i.e., [^{3}H]-DPCPX or [^{3}H]-LUF5962. Seven compounds, excluding FSCPX, had KRI values ≥ 1.2 with [^{3}H]-DPCPX as the radioligand, which indicated that these compounds dissociated more slowly from the receptor than [^{3}H]-DPCPX (Figure 3.5, white bars). KRI values for the same panel

of unlabeled ligands against [^{3}H]-LUF5962 were also determined (Figure 3.5, gray bars). In the latter situation all compounds displayed a KRI < 1.2, except FSCPX, since the radioligand used ([^{3}H]-LUF5962) has a relatively slow off-rate (0.021 min^{-1}). Interestingly, most of the compounds adopted a concerted trend with a decreased KRI value compared to that obtained with [^{3}H]-DPCPX. This is in accordance with the observation that indeed most compounds have faster dissociation rates than LUF5962 as determined by full kinetic experiments with [^{3}H]-DPCPX (Table 3.2). For validation of the dual-point assay, four compounds with lower or similar KRI values (compared to DPCPX, KRI ≤ 1) and four compounds with higher KRI values (≥1.2) were further characterized in follow-up kinetic assays (Table 3.2).

Subsequently, competition association assays in the presence of [^{3}H]-DPCPX were performed to determine the binding kinetics of the eight compounds that had divergent KRI values (Table 3.2). In the present chapter, we used FSCPX as a tool compound, which had a KRI value of 5.4 ± 1.2 at the hA_1R, indicative of negligible dissociation (Table 3.2 and Figure 3.4A). Similarly to FSCPX, the specific binding of [^{3}H]-DPCPX in the presence of unlabeled LUF5962 (compound **31**) became biphasic, which was represented by a decline towards equilibrium after a typical 'overshoot' (Figure 3.6A). Its dissociation rate was 0.021 ± 0.005 min^{-1}, which was approximately ten times slower than DPCPX's dissociation rate (Table 3.2). Next to that, we also decided to radiolabel this slow off-rate compound, which enabled us to directly determine its off-rate in a classic kinetic dissociation experiment. This assay yielded a dissociation rate of 0.025 ± 0.002 min^{-1}, which was in good agreement with the off-rate determined from the competition association assay (Table 3.1). In addition, this matched with its KRI value of 1.6 ± 0.4 determined in the dual-point screening method against [^{3}H]-DPCPX. Subsequent KRI screening with [^{3}H]-LUF5962 of the same set of compounds also supported our hypothesis that a KRI-value above 1.2 indicates a relatively slow dissociation from the target, while a lower KRI-value predicts a relatively fast dissociation rate. Moreover, additional kinetic experiments of other A_1R antagonists proved that the obtained KRI values were a good predictor for their off-rates (Table 3.2). The three other selected compounds with KRI values bigger than 1.2 (**32**: 2.0 ± 0.4, **33**: 1.6 ± 0.4 and **35**: 1.2 ± 0.3) had dissociation rates of 0.027 ± 0.004 min^{-1}, 0.038 ± 0.010 min^{-1} and 0.088 ± 0.003 min^{-1}, respectively. Next, four compounds (**7**, **13**, **19** and **22**) with KRI values ranging from 0.57 to 1.0 were selected for further characterization of the methodology. As expected, all four compounds had faster or similar off-

Table 3.2 | Kinetics rate indexes (KRI) and binding kinetics obtained from the dual-point or standard competition association assay of DPCPX, FSCPX and representative hA_1R antagonists.

Cmpd	*KRI*[a]	k_{on} *(nM^{-1}·min^{-1})*[b]	k_{off} *(min^{-1})*[b]	*RT (min)*[c]	*Kinetic K_D (nM)*[d]	K_i *(nM)*[e]
DPCPX	1.0 ± 0.1	0.14 ± 0.02	0.25 ± 0.01	4.0 ± 1.0	1.8 ± 0.3	2.3 ± 0.3
FSCPX	5.4 ± 1.2	0.0037 ± 0.0010	0.0010 ± 0.0002	1000 ± 33	0.27 ± 0.09	5.7 ± 1.0
LUF5962 (**31**)	1.6 ± 0.1	0.060 ± 0.010	0.021 ± 0.005	48 ± 12	0.35 ± 0.08	0.24 ± 0.03
32	2.0 ± 0.4	0.042 ± 0.006	0.027 ± 0.004	37 ± 6	0.64 ± 0.10	0.73 ± 0.07
33	1.6 ± 0.4	0.0012 ± 0.0004	0.038 ± 0.010	26 ± 11	32 ± 14	25 ± 5
35	1.2 ± 0.3	0.0043 ± 0.0007	0.088 ± 0.003	11 ± 2	20 ± 3	36 ± 4
7	0.57 ± 0.10	0.48 ± 0.10	3.0 ± 0.9	0.33 ± 0.10	6.3 ± 2.3	9.4 ± 3.0
13	1.0 ± 0.1	0.13 ± 0.07	0.57 ± 0.20	2.0 ± 0.7	4.4 ± 3.0	8.3 ± 0.2
19	0.89 ± 0.10	0.62 ± 0.05	0.68 ± 0.10	1.0 ± 0.2	1.1 ± 0.2	1.1 ± 0.2
22	0.73 ± 0.20	0.10 ± 0.01	0.29 ± 0.01	3.0 ± 0.2	2.9 ± 0.2	4.9 ± 2.0

Values are means ± s.e.m of at least three independent experiments performed in duplicate. [a] Kinetic rate indexes (KRI) were determined in the dual-point competition association assay. [b] k_{on} (k_3), k_{off} (k_4) of unlabeled antagonists values were determined in [^{3}H]-DPCPX (2.5 nM) competition association assay at 25 ˚C. [c] RT (residence time) = 1 / k_{off}. [d] Kinetic K_D = k_{off} / k_{on}. k_{on} (k_3) and k_{off} (k_4) values of unlabeled antagonists were generated from [^{3}H]-DPCPX (2.5 nM) competition association assay association assays at 25˚C. [e] K_i values were from displacement assays at 25 ˚C or obtained from Chang *et al.* and Van Veldhoven *et al.*[17,18]

rates compared to DPCPX (Table 3.2). Typically, [^{3}H]-DPCPX association in the presence of a 'fast' compound such as **7** (Figure 3.5, for its structure) resulted in a slow monophasic ascent of radioligand binding, indicative of a faster dissociation from the receptor than [^{3}H]-DPCPX (Figure 3.6A). Its dissociation rate was determined as 3.0 ± 0.9 min^{-1}, which was more than ten times faster than that of the radioligand. Notably, a good correlation (Figure 3.6B, r^2 = 0.8511, P < 0.0005) was observed between the negative logarithm of the ligands' dissociation rates (pk$_{off}$), excluding that of FSCPX (considering its unique irreversible binding character), and their KRI values derived from our new kinetic screening method. No significant correlation was observed between the negative logarithm of the ligands' association rates (pk$_{on}$) and their KRI values (r^2 = 0.2551, P = 0.1655). This further proved that the KRI value is a good predictor for a ligand's dissociation rate in the dual-point assay.

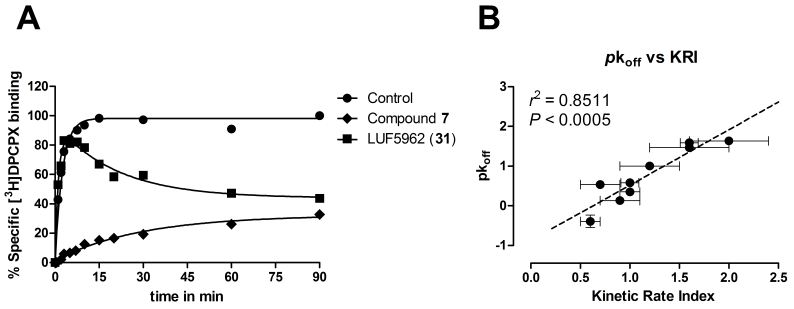

Figure 3.6 | Panel A: Competition association assay of [^{3}H]-DPCPX in the absence or presence of two unlabeled representative hA$_1$R antagonists. LUF5962 (**31**) and compound **7** were found in a dual-point screening assay to have kinetic rate indexes of 1.6 ± 0.1 and 0.57 ± 0.10, respectively. Association and dissociation rates for unlabeled ligands were calculated by fitting the data in the competition association model as in Equation 7.[11] Representative graph from one experiment performed in duplicate. Panel B: Correlation between the negative logarithm of the ligands' dissociation rates (pk_{off}) and their kinetic rate index (KRI) values derived from dual-point competition association assay (r^2 = 0.8511, P < 0.0005). Data used in this plot are detailed in Table 3.2 (excluding FSCPX, see text). Data are expressed as mean ± s.e.m from three independent experiments.

Advantages of the dual-point competition association assay and its future application in kinetic binding screening

Currently, there are several assays available developed for kinetics screening. For instance, Heise *et al.* developed a scintillation proximity assay (SPA) to measure K_i values for gonadotropin-releasing hormone receptor (GnRH receptor) antagonists after 30 min and 10 h incubation.[22] This assay is based on the observation that a slowly dissociating compound will display a decrease of apparent K_i value over time, since it requires a longer incubation time to reach equilibrium.[11,22] Another methodology is a functional assay described by Morriello *et al.*, where hNK$_1$R overexpressing CHO cells were pretreated with neurokinin 1 receptor (NK$_1$R) antagonists before a measurement of the remaining activity induced by subsequently added substance P (endogenous agonist of hNK$_1$R). A complete reversal of the hNK$_1$R antagonism indicated a short receptor residence time of the compound under evaluation, while

an insurmountable effect of the tested ligand suggested longer receptor occupancy. In such a way, the recovery of the response to substance P gave an indication of an antagonist's receptor off-rate.[23] Similarly, the dual-point assay and its resulting KRI values described in the present chapter allow for a fast selection of long receptor residence time compounds, e.g., compound **31** in the present chapter. Importantly, our new methodology has advantages over other assays. Firstly, as it only needs two assay points for testing one compound, the efficiency of kinetic screening is increased. Secondly, the KRI value derived from this assay yields direct information of a ligand's binding kinetics, thus it allows for discrimination between fast, slowly and very slowly dissociating compounds. Moreover, this assay also provides the ability to identify ligands with short receptor residence times (i.e., compounds with KRI values lower than 1). In terms of therapies that need enduring target occupancy and a long-acting biological efficiency, a slowly dissociating compound might be an appropriate strategy for a clinical application. An example of a marketed long-residence-time drug is candesartan, which is an angiotensin II type 1 (AT_1) receptor antagonist. Its enhanced long-lasting blood pressure lowering effects have been attributed to a slow receptor off-rate; they even persist after the candesartan plasma concentration has become undetectable.[24,25] In contrast, when an endogenous ligand has ubiquitous physiological functions, a rapidly dissociating exogenous ligand might be preferred to prevent the concomitant mechanism-based, on-target toxicity. An example is the short-lived intervention of dopamine-2 receptor (D_2 receptor) activity by clozapine. Its 'atypical', short receptor residence time is thought to prevent adverse effects caused by lasting occupation of striatal D_2 receptors, which respond to fast fluctuations in the local dopamine concentration.[26,27] Importantly, the dual-point assay and the KRI value could be employed to select both slowly and rapidly dissociating compounds (i.e., compound **31** and **7**). This versatility underscores its usability in future early phase drug discovery.

As represented in Figure 3.5, the same set of unlabeled A_1 receptor ligands have different KRI values if tested against two kinetically different radioligands. Indeed, since the dual-point approach and its derived KRI are mainly based on whether an unlabeled competitor dissociates faster or slower from its target than a particular radioligand, the choice of radioligand becomes the key for a reliable kinetic screening. Here we propose that the choice for an 'ideal' radioligand (if one has the luxury of a number of radioligands) should take into account the drug target and the particular screening purpose. More

specifically, if one searches for slowly dissociating compounds, a relatively long residence time radioligand would be preferred, while for short residence time compounds, a relatively fast dissociating radioligand may be needed. By following this principle the load of follow-up kinetic determinations for selected compounds can be reduced. However, it is also necessary to take the assay practicability into consideration. In the present chapter, for instance, LUF5962 has a slow off-rate. According to Equation 5 regarding the t_1 time point set-up, it would require nearly two hours for [^{3}H]-LUF5962 to reach equilibrium when a concentration of one-fold its K_i value (0.24 nM) is used. Logically, this results in an even later t_2 time point. Thus, we applied 1.0 nM [^{3}H]-LUF5962 (approximately four time its K_i) in our additional KRI experiments, enabling a relatively quick t_1 at approximately 30 min and the same t_2 as for [^{3}H]-DPCPX (120 min). The robustness of the dual-point competition assay is underscored by the fact that even a less than ideal radioligand, such as [^{3}H]-LUF5962, can still be used for screening purposes.

In the present chapter, we have merely described the application of the dual-point assay for a prototypical GPCR target, namely the adenosine A_1R. We believe that this assay can have a more general application for other drug targets as well. This consideration is supported by an increasing amount of studies that characterized receptor binding kinetics, such as for the histamine H_1 receptor, the corticotropin-releasing factor type-1 receptor (CRF_1R) and more recently the adenosine A_{2A} receptor, where Motulsky and Mahan's theory and their competition association assay were used.[28-30] Similar patterns of competition association curves were observed in these studies, i.e., in the presence of a fast dissociating competitor the specific radioligand binding approached equilibrium slowly; while in the presence of a slowly dissociating compound, it showed firstly the typical 'overshoot' followed by a constant decline to a plateau as in Figure 3.3B. This, as a proof-of-concept, implies the feasibility of a dual-point kinetic screening and the use of KRI for searching desired leads on other drug targets as well.

In summary, the dual-point competition association assay is a valid tool to perform fast and high-throughput screening for compounds having either long or short residence times. The KRI value, which we coined in the present chapter, is an effective predictor of a compound's dissociation rate from its target. We believe that this approach can be of general use at other drug targets, e.g., other GPCRs, after assay optimization for individual receptors.

References:

1. Zhang, R.; Monsma, F. The importance of drug-target residence time. *Curr Opin Drug Discov Devel* 2009, 12, 488-496.
2. Zhang, R.; Monsma, F. Binding kinetics and mechanism of action: toward the discovery and development of better and best in class drugs. *Expert Opin Drug Discov* 2010, 5, 1023-1029.
3. Swinney, D. C. Biochemical mechanisms of drug action: what does it take for success? *Nat Rev Drug Discov* 2004, 3, 801-808.
4. Copeland, R. A.; Pompliano, D. L.; Meek, T. D. Drug-target residence time and its implications for lead optimization. *Nat Rev Drug Discov* 2006, 5, 730-739.
5. Anthes, J. C.; Gilchrest, H.; Richard, C.; Eckel, S.; Hesk, D.; West, R. E.; Williams, S. M.; Greenfeder, S.; Billah, M.; Kreutner, W.; Egan, R. E. Biochemical characterization of desloratadine, a potent antagonist of the human histamine H_1 receptor. *Eur J Pharmacol* 2002, 449, 229-237.
6. Copeland, R. A. Evaluation of enzyme inhibitors in drug discovery: a guide for medicinal chemists and pharmacologists. *Methods Biochem Anal* 2005, 46, 1-265.
7. Ojima, M.; Inada, Y.; Shibouta, Y.; Wada, T.; Sanada, T.; Kubo, K.; Nishikawa, K. Candesartan (CV-11974) dissociates slowly from the angiotensin AT_1 receptor. *Eur J Pharmacol* 1997, 319, 137-146.
8. Casarosa, P.; Kollak, I.; Kiechle, T.; Ostermann, A.; Schnapp, A.; Kiesling, R.; Pieper, M.; Sieger, P.; Gantner, F. Functional and biochemical rationales for the 24-Hour long duration of action of olodaterol. *J Pharmacol Exp Ther* 2011, 337, 600-609.
9. Dowling, M. R.; Charlton, S. J. Quantifying the association and dissociation rates of unlabelled antagonists at the muscarinic M_3 receptor. *Br J Pharmacol* 2006, 148, 927-937.
10. Packeu, A.; Wennerberg, M.; Balendran, A.; Vauquelin, G. Estimation of the dissociation rate of unlabelled ligand-receptor complexes by a 'two-Step' competition binding approach. *Br J Pharmacol* 2010, 161, 1311-1328.
11. Motulsky, H. J.; Mahan, L. C. The kinetics of competitive radioligand binding predicted by the law of mass action. *Mol Pharmacol* 1984, 25, 1-9.
12. Fredholm, B. B.; IJzerman, A. P.; Jacobson, K. A.; Klotz, K. N.; Linden, J. International Union of Pharmacology. XXV. Nomenclature and Classification of Adenosine Receptors. *Pharmacol Rev* 2001, 53, 527-552.
13. Fredholm, B. B.; IJzerman, A. P.; Jacobson, K. A.; Linden, J.; Müller, C. E. International Union of Basic and Clinical Pharmacology. LXXXI. Nomenclature and Classification of Adenosine Receptors--an Update. *Pharmacol Rev* 2011, 63, 1-34.
14. Jacobson, K. A.; Gao, Z. G. Adenosine receptors as therapeutic targets. *Nat Rev Drug Discov* 2006, 5, 247-264.
15. Gao, Z. G.; Jacobson, K. A. Emerging adenosine receptor agonists. *Expert Opin Emerg Drugs* 2007, 12, 479-492.
16. Van Muijlwijk-Koezen, J. E.; Timmerman, H.; Van der Sluis, R. P.; Van de Stolpe, A. C.; Menge, W. M.; Beukers, M. W.; Van der Graaf, P. H.; De Groote, M.; IJzerman, A. P. Synthesis and use of FSCPX, an irreversible adenosine A_1 antagonist, as a 'receptor knock-down' tool. *Bioorg Med Chem Lett* 2001, 11, 815-818.
17. Chang, L. C.; Spanjersberg, R. F.; Von Frijtag Drabbe Kunzel, J. K.; Mulder-Krieger, T.; Brussee, J.; IJzerman, A. P. 2,6-disubstituted and 2,6,8-trisubstituted purines as adenosine receptor

antagonists. *J Med Chem* 2006, 49, 2861-2867.

18. Van Veldhoven, J. P.; Chang, L. C.; von Frijtag Drabbe Kunzel, J. K.; Mulder-Krieger, T.; Struensee-Link, R.; Beukers, M. W.; Brussee, J.; IJzerman, A. P. A new generation of adenosine receptor antagonists: from di- to trisubstituted aminopyrimidines. *Bioorg Med Chem* 2008, 16, 2741-2752.
19. Smith, P. K.; Krohn, R. I.; Hermanson, G. T.; Mallia, A. K.; Gartner, F. H.; Provenzano, M. D.; Fujimoto, E. K.; Goeke, N. M.; Olson, B. J.; Klenk, D. C. Measurement of protein using bicinchoninic acid. *Anal Biochem* 1985, 150, 76-85.
20. Cheng, Y., Prusoff, W. H. Relationship between the inhibition constant (K_I) and the concentration of inhibitor which causes 50 percent inhibition (I_{50}) of an enzymatic reaction. *Biochem Pharmacol* 1973, 22, 3099-3108.
21. Heitman, L. H.; Mulder-Krieger, T.; Spanjersberg, R. F.; von Frijtag Drabbe Kunzel, J. K.; Dalpiaz, A.; IJzerman, A. P. Allosteric modulation, thermodynamics and binding to wild-Type and mutant (T277A) adenosine A_1 receptors of LUF5831, a novel nonadenosine-Like agonist. *Br J Pharmacol 2006,* 147, 533-541.
22. Heise, C. E.; Sullivan, S. K.; Crowe, P. D. Scintillation proximity assay as a high-throughput method to identify slowly dissociating nonpeptide ligand binding to the GnRH receptor. *J Biomol Screen* 2007, 12, 235-239.
23. Morriello, G. J.; Chicchi, G.; Johnson, T.; Mills, S. G.; Demartino, J.; Kurtz, M.; Tsao, K. L.; Zheng, S.; Tong, X.; Carlson, E.; Townson, K.; Wheeldon, A.; Boyce, S.; Collinson, N.; Rupniak, N.; Devita, R. J. Fused tricyclic pyrrolizinones that exhibit pseudo-irreversible blockade of the NK_1 receptor. *Bioorg Med Chem Lett* 2010, 20, 5925-5932.
24. Fuchs, B.; Breithaupt-Grogler, K.; Belz, G. G.; Roll, S.; Malerczyk, C.; Herrmann, V.; Spahn-Langguth, H.; Mutschler, E. Comparative pharmacodynamics and pharmacokinetics of candesartan and losartan in man. *J Pharm Pharmacol* 2000, 52, 1075-1083.
25. Nunez, S.; Venhorst, J.; Kruse, C. G. Target-drug interactions: first principles and their application to drug discovery. *Drug Discov Today* 2012, 17, 10-22
26. Kapur, S.; Seeman, P. Ketamine has equal affinity for NMDA receptors and the high-affinity state of the dopamine D_2 receptor. *Biol Psychiatry* 2001, 49, 954-957
27. Schneider, L. S.; Dagerman, K.; Insel, P. S. Efficacy and adverse effects of atypical antipsychotics for dementia: meta-analysis of randomized, placebo-controlled trials. *Am J Geriatr Psychiatry* 2006, 14, 191-210.
28. Slack, R. J.; Russell, L. J.; Hall, D. A.; Luttmann, M. A.; Ford, A. J.; Saunders, K. A.; Hodgson, S. T.; Connor, H. E.; Browning, C.; Clark, K. L. Pharmacological characterization of GSK1004723, a novel, long-acting antagonist at histamine H_1 and H_3 receptors. *Br J Pharmacol* 2011, 164, 1627-1641.
29. Ramsey, S. J.; Attkins, N. J.; Fish, R.; van der Graaf, P. H. Quantitative pharmacological analysis of antagonist binding kinetics at CRF_1 receptors *In vitro* and *In vivo*. *Br J Pharmacol* 2011, 164, 992-1007
30. Guo, D.; Mulder-Krieger, T.; IJzerman, A. P.; Heitman, L. H. Functional efficacy of adenosine A_{2A} receptor agonists is positively correlated to their receptor residence time. *Br J Pharmacol* 2012, 166, 1846-1859
31. Martinson, E. A.; Johnson, R. A.; Wells, J. N. Potent adenosine receptor antagonists that are selective for the A_1 receptor subtype. *Mol Pharmacol* 1987, 31, 247–52
32. Williams, M.; Braunwalder, A.; Erickson, T. J. Evaluation of the binding of the A_1 selective adenosine radioligand, cyclopentyladenosine (CPA), to rat brain tissue. *N-S Arch Pharmacol* 1986, 332, 179–83.